

Figure 2. Shape of a 21-bead Rouse chain in uniaxial extension at a dimensionless extension rate of 0.45. See the text for more details.

along the horizontal axis. In Figure 2, the principal axis of extension is aligned along the horizontal axis. In both figures, a circle of radius 1.0 corresponds to the shape of the molecular envelope at equilibrium.

The "dumbbell" shape of the envelopes reveals the difficulty in using the perpendicular low-angle scattering dimension to infer a characteristic transverse length for the stretched molecule. At higher extension rates, where the Rouse model is a less useful depiction of a real mac-

romolecule, the dumbbell shape becomes even sharper. Part of the reason that the scattering approach leads to dumbbell shapes is that averaging is conducted as the second moment of center-of-mass coordinates integrated over all beads in a chain. Different averaging procedures, which may not be experimentally accessible, may provide more intuitive, nearly ellipsoidal shapes under the same conditions.² The results presented here should not be considered unique to the chosen model, and we expect that dumbbell shapes will be obtained for polymers which are not closely described by the Rouse formulation. Scattering experiments of the type discussed here have been previously reported,³ and a calculation of scattering in shear flow has been derived previously.⁴ Our model, valid only in the small-angle limit, is much simpler and applicable to a broader class of flows. A more accurate description would also consider the effects of hydrodynamic interactions, but the incorporation of nonequilibrium hydrodynamic interactions would appear extremely complex. We have recently become aware of a previous derivation of eq 11 by Roitman and Schrag.⁵

References and Notes

- (1) Bird, R. B.; Curtiss, C. F.; Armstrong, R. C.; Hassager, O. *Dynamics of Polymeric Liquids. Vol. 2. Kinetic Theory*, 2nd ed.; Wiley: New York, 1987; Chapter 15.
- (2) Hoagland, D. A.; Prud'homme, R. K., submitted for publication in *J. Non-Newtonian Fluid Mech.*
- (3) (a) Cottrell, F. R.; Merrill, E. W.; Smith, K. A. *J. Polymer Sci., Part A-2* 1969, 7, 1415. (b) Smith, K. A.; Merrill, E. W.; Peebles, L. H.; Banijamali, S. H. In *Polymères et Lubrification*; C. Wolf, organizer; Colloques Internationaux du CNRS, No. 233; CNRS: Paris, 1975; p 341. (c) Lindner, P.; Oberthur, R. C. *Colloid Polym. Sci.* 1985, 263, 443.
- (4) Peterlin, A.; Reinhold, C. *J. Chem. Phys.* 1964, 40, 1029.
- (5) Roitman, D. B.; Schrag, J. L. In *Polymer-Flow Interaction*; Rabin, Y., Ed.; American Institute of Physics Conference Proceedings, No. 137; AIP: New York, 1985; p 77.

Communications to the Editor

New Three-Dimensional Structure for A-Type Starch

Starch granules are the major form for packaging storage carbohydrates in green plants. Most granules exhibit a natural crystallinity due to the local arrangement of linear amylose fragments ($\alpha(1\rightarrow4)$ -linked D-glucopyranosyl units), which correspond to the branches of amylopectin, a treelike polymer.^{1,2} Two different X-ray patterns can be obtained according to the origin of the granules: A type from cereals and B type from tubers. Previous structural studies on A-type starch have yielded contradictory results: crystallographic data on artificial fibers of amylose resulted in a structure based on antiparallel packing of right-handed double helices,³ while biochemical data can accommodate only parallel molecules.^{4,5}

New crystallographic data were obtained by using two different but interrelated methods: deconvolution of X-ray powder patterns into individual peaks⁶ (Figure 1) and electron diffraction on single micron-sized crystals⁷ (Figure 2). Samples were prepared by recrystallizing amylose fractions, with a degree of polymerization (DP) of 15, under conditions where the growth of A-type crystals is favored. X-ray diagrams recorded for both samples (polycrystalline powder for X-ray diffraction and micron-sized crystals for electron diffraction) were similar to those displayed by

Table I
Comparison of Cell Dimensions Obtained by Different Diffraction Methods^a

	orthorhombic cell			monoclinic ^b
	fiber X-ray ³	microcrystal electrons	powder X-ray	cell powder X-ray
a, nm	1.190	1.116	1.172	2.1245
b, nm	1.770	1.751	1.772	1.172
c, nm	1.052	1.045	1.068	1.068
α , deg	90	90	90	90
β , deg	90	90	90	90
γ , deg	90	90	90	123.48
V, nm ³	2.216	2.042	2.218	2.218
T, °C	20	-170	20	20

^a The orthorhombic-like cell does not show significant variations from powder and fiber data. However, the electron diffraction data yield a smaller cell; this can be explained by a contraction of the cell due to the very low experimental temperature. ^b The monoclinic cell is deduced by an appropriate transformation of the orthorhombic-like cell derived from the X-ray powder data.

native starch granules but were better resolved. These two new sets of diffraction data, along with that reported by Wu and Sarko³ yielded the same orthorhombic-like cell (Table I), having a volume of about 2.2 nm³. According to the measured density of the synthetic crystals, which agrees with the reported density of the fiber, 12 glucose

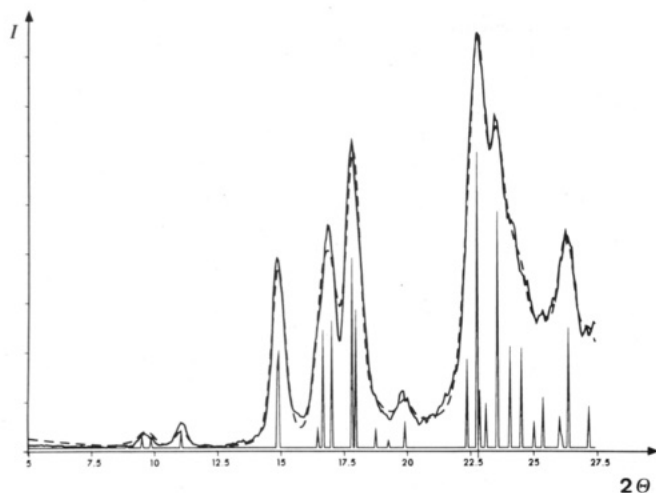


Figure 1. X-ray powder pattern of A-amylose (—) together with its deconvolution into individual diffraction peaks and the calculated intensity peak envelopes (---). Amylose fractions with DP 15 were obtained by mild hydrolysis of potato starch¹⁵ and solubilized in hot water. A-type crystalline powder was precipitated by addition of hot acetone. The crystals were collected and washed by successive centrifugations in a mixture of water and acetone (50/50 v/v). They were mounted in a chamber maintained at a relative humidity of 90% on a CGR Sigma 2080 diffractometer. The diagram was recorded with a scintillation counter by using the Cu K α X-ray radiation ($\lambda = 0.154$ nm). After Lorentz-polarization corrections, the position, intensity, and shape of individual peaks were resolved by a new decomposition method,¹⁷ using a Pearson VII type function and a unit-cell refinement coupled with an optimization algorithm. This program was especially written for diffraction diagrams of poor resolution, such as obtained with many biopolymers.

residues together with a few possible water molecules can be accommodated in the unit cell.

The amount of diffraction data is not sufficient to attempt a structure elucidation through conventional crystallographic methods. In such a case, one can only proceed by building structural models by conformational analysis methods and then testing the predictions based on these models against experimental data. For an observed fiber repeat c of 1.068 nm, computer modeling on $\alpha(1\rightarrow4)$ linked glucose units indicated that the most extended conformations of the linkage would give a repeat of the amylose oligomer with DP = 3 (maltotriose) while a shallower one could give a maltohexaose (DP = 6). On the assumption that homopolymers have a regular helical conformation,⁸ three possibilities were tested against their packing constraints: (1) four single 3-fold helices, (2) two single 6-fold helices, and (3) two double 6-fold helices repeating $2c = 2.136$ nm but separated by a 2-fold axis which restores the observed repeat of 1.068 nm. The first hypothesis can be readily discarded through computation of intrachain energy, and in the second case it is impossible to pack two 6-fold helices into the unit cell because of numerous short interchain contacts. The only remaining hypothesis is that of the double-parallel-stranded helix, either left or right handed. Data on other polysaccharides⁹ would tend to favor the occurrence of a left-handed chirality, such as the one proposed by French.¹⁰ The conformation of the glycosidic linkage, derived from modeling a left-handed single helix from the observed fiber repeat, corresponds to one of the stable energy minima calculated for maltose (DP = 2) whereas the conformation derived from modeling a right-handed helix is less favored on an energy ground.¹¹ The left-handed conformation is also reminiscent of the one observed in a crystalline linear amylosic oligomer.¹² Assembling two such parallel single strands through a

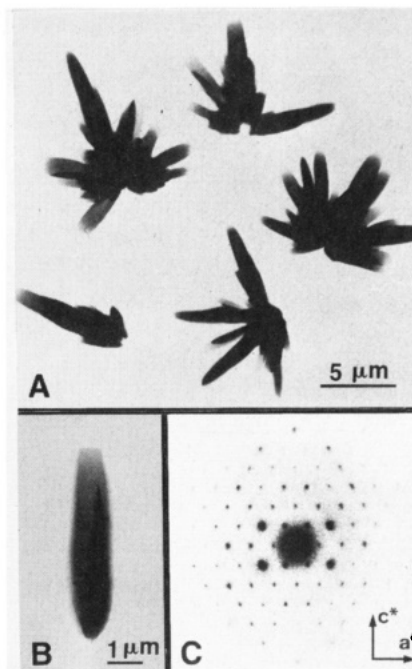


Figure 2. Electron micrographs and electron diffraction diagram of micron-sized crystals of A-amylose. For the preparation of the crystals, amylose fraction of DP 15 in aqueous solutions were prepared as previously described (see legend of Figure 1). These solutions were warmed up to 60 °C and subjected to acetone vapors for 12 h. A-amylose crystals which precipitated were collected and washed in a mixture of acetone and water (50/50 v/v). Typical crystals occurred as platelet aggregates organized in a rosette-like fashion (A). Each platelet is a monocrystal (B) with dimension $10 \times 1 \times 0.3$ μm . Such crystals can be analyzed by electron diffraction (C). For this purpose, grids supporting the crystals were equilibrated in a desiccator where a relative humidity of 97% was maintained. They were then examined under frozen hydrated conditions with a Phillips EM400T electron microscope, operating at 120 KV and low dose conditions.¹⁶ The diagram presented in (C) corresponds to the a^*c^* projection of the reciprocal lattice of A-amylose; it was obtained by tilting the crystal by 36° about its long axis, identified as being aligned with the c axis of the unit cell.

2-fold symmetry operation permits formation of a double helix having no short contacts. Furthermore, interstrand stabilization is achieved through hydrogen bonding.

Electron diffraction data provided the symmetry elements relating two such double helices in the unit cell. Throughout the experimentally accessible reciprocal lattice, the diffraction diagrams, as the one represented in Figure 2C, exhibit systematic absences of reflections with indices $h + k + l = 2n + 1$, indicating a body-centred lattice. The possible orthorhombic space groups have too many symmetry requirements for accommodating two such chiral entities. The only solution is the face-centered monoclinic space group $B2$ (with the fiber axis c as the unique axis), after adequate transformation of the cell axes a and b . Electron diffraction data provided proof of monoclinic symmetry. By sequential tilting about an axis perpendicular to the crystal axis, some hkl and $-hkl$ (in the orthorhombic denomination) reflection intensities could be compared and were found to be unequal, contrary to expectations for an orthorhombic space group. In the monoclinic cell, the two double helices are located respectively at the corners of the cell and in the middle of the faces (a,c) (on 2-fold axes) and are related by a simple translation $a/2 + c/2$ (Figure 3). This monoclinic space group, which is the only one to be consistent with the set of observed systematic absences, can accommodate only parallel double helices.

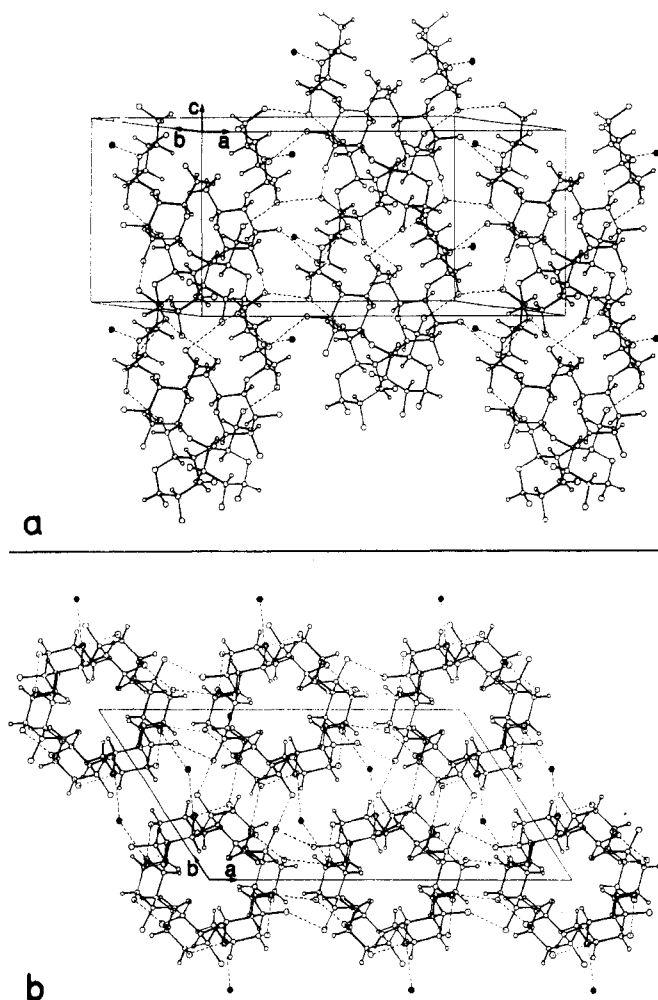


Figure 3. Two projection views of the double helices of A-amylose and of the four water molecules (as black spots) in one unit cell. (a) Meridional projection of the face (a,c) with the center chain translated by $c/2$ and $a/2$ from the corner chains. (b) Equatorial projection on the face (a,b). The polysaccharide structure, without water, refined with the LALS program¹³ yields good R factors (0.26 and 0.29 for fiber and powder data, respectively) and no serious short contact was found between the chains. Further contact energy and X-ray refinement gave the localization of the four water molecules. The final R factor in three dimensions is 0.25 for fiber diffraction intensities and 0.27 for powder diffraction intensities. The final structure is characterized by numerous hydrogen bonds (represented as dashed lines) between the chains and the water molecules and between the molecules of different chains also. The drawing was created with the PITMOS program.¹⁷

In the last step of this study, the model was checked against both packing constraints and experimental data. The refinement of the three $\alpha(1\rightarrow4)$ linkage conformations and of the rotation of the double helices was performed with the help of the LALS program¹³ (linked-atom least-squares reciprocal space refinement system) which combines X-ray and contact refinements. Calculations were performed in three independent runs (1) with contact energy values, (2) with c diffraction intensity data from the fiber, and (3) with data from the powder. These three refinements converged to the same structure with good reliability factors (R factors) and no serious short contacts between the chains. Comparison between calculated and measured density suggested the presence of four water molecules per unit cell. Further refinement indicated that these molecules are located between the amylosic chains, where there is sufficient space to accommodate them (see Figure 3).

All crystalline samples of amylose studied here, i.e.,

synthetic crystals, polycrystalline powders, and artificial fibers, exhibit the same scattering features and therefore the same crystal and molecular organization as the crystalline components of native starch. The formation of double-helical structures involving short amylose chains appears to be a ubiquitous phenomenon governed either by biosynthesis (in the starch granule) or by simple thermodynamic rules (in solution). The single-strand conformation can be predicted from the conformational energy map of the $\alpha(1\rightarrow4)$ linkage.¹¹ The formation of such double helices in solution has been postulated to explain two major properties of starch: gelatinization and retrogradation.¹⁴

The size of short branches of amylopectin (12–20 glucose residues for wheat starch) is ideal for the formation of double helices; these chains are densely packed in crystallites arranged radially in the granule. Therefore, the three-dimensional structure of amylose A, or more precisely of the linear branches of amylopectin in A-type starch, is consistent with the "cluster" model of amylopectin⁵ as well as with the overall architecture of the starch granule.¹

Registry No. Starch, 9005-25-8; amylose, 9005-82-7.

References and Notes

- (1) Lineback, D. R. *J. Jpn. Soc. Starch Sci.* **1986**, *33*, 80–88.
- (2) Robin, J. P.; Mercier, C.; Charbonnière, R.; Guilbot, A. *Cereal Chem.* **1974**, *51*, 389–406.
- (3) Wu, H. C. H.; Sarko, A. *Carbohydr. Res.* **1978**, *61*, 27–40.
- (4) Duprat, F.; Gallant, D.; Guilbot, A.; Mercier, C.; Robin, J. P. In *Les Polymères Végétaux*; Monties, B., Ed.; Gauthier-Villars: Paris, 1980; pp 176–229.
- (5) Manners, D. J.; Matheson, N. K. *Carbohydr. Res.* **1981**, *90*, 99–110.
- (6) Buléon, A.; Duprat, F.; Booy, F. P.; Chanzy, H. *Carbohydr. Polym.* **1984**, *4*, 161–173.
- (7) Tran, V.; Buléon, A. *J. Appl. Crystallogr.*, in press.
- (8) Natta, G.; Corradini, P. *J. Polym. Sci.* **1959**, *39*, 29–46.
- (9) Pérez, S.; Vergelati, C. *Biopolymer* **1985**, *24*, 1809–1822.
- (10) French, A. D.; Murphy, V. G. *Cereal Food World* **1977**, *22*, 61–70.
- (11) Pérez, S.; Vergelati, C. *Polym. Bull.* **1987**, *17*, 141–148.
- (12) Pangborn, W.; Langs, D.; Pérez, S. *Int. J. Biol. Macromol.* **1985**, *7*, 363–369.
- (13) Smith, P. J. C.; Arnott, S. *Acta Crystallogr., Sect. A* **1978**, *A34*, 3–11.
- (14) Matsukura, U.; Matsunaga, A.; Kainuma, K. *J. Jpn. Soc. Starch Sci.* **1983**, *30*, 106–113.
- (15) Robin, J. P. Ph.D. Thesis, Paris, 1976.
- (16) Chanzy, H.; Guizard, C.; Vuong, R. *J. Microscopy* **1977**, *111*, 143–150.
- (17) Pérez, S.; Scaringe, R. P. *J. Appl. Crystallogr.* **1986**, *19*, 65–66.

[†] Affiliated to the Université Scientifique, Technologique et Médicale de Grenoble, France.

Anne Imberty,* Henri Chanzy, and Serge Pérez

Centre de Recherches sur les Macromolécules
Végétales,† C.N.R.S., B.P. 68
F-38402 Saint-Martin d'Hères, France

Alain Buléon and Vinh Tran

Laboratoire de Physico-Chimie des Macromolécules
I.N.R.A., F-44072 Nantes, France

Received March 5, 1987;

Revised Manuscript Received June 8, 1987

Broken Worm and Wormlike Models for Polyisocyanates

In a recent publication¹ we discussed the effect of pendant group structure on the axial dimension of polyisocyanates. It was established that poly[(S)-(2,2-di-